Chapter 4

Spots position

4.1 Foreword

In the previous chapter we addressed the problem of the footprint morphology or, in other words, the problem of its general shape. We saw that the answer to the question "What does the Io footprint look like?" is already telling us a lot about the ongoing processes that connect Io to its parent planet. The footprint is composed of at least three spots (sometimes merged) followed by a long trailing tail. The multiplicity of the spots excludes the simplest unipolar inductor model, but the evolution of the spots position cannot be solely explained by reflections of Alfvén waves. We have proposed a new interpretation to explain the evolution of the IFP morphology and to reconcile the occurrence of the different IFP spots with the observation of electron beams at Io. We now continue our endeavor by answering another basic question: "What is the Io footprint location?". Of course, this question will immediately be followed by a recurrent questioning in this thesis: "What is it telling us about the Io-Jupiter interaction?".

We have seen in the introductory chapter that the Io footprint is a consequence of the interaction between Io and the Jovian magnetosphere and that the perturbation generated at Io propagates along the magnetic field lines convecting along Io. The position of the IFP thus contains two pieces of information. First, whatever the far field interaction model we consider, the IFP is connected to field lines crossing Io's orbit. If we extend this observation to the whole IFP footpath, i.e. the locus of the IFP, and to the other satellites footpaths as well, then we can conclude that any accurate Jovian magnetic field model should link the field lines crossing any satellite orbit to the corresponding footpath. Consequently, the position of the

satellite footprints on Jupiter is of particular importance because they can be used to constrain magnetic field models.

However, all the models describing the Io-Jupiter interaction predict that the footprint is not exactly located at the foot of the unperturbed field lines passing through Io but should lie a few degrees downstream. More interestingly, the different models do not agree on how far downstream the auroral emission should appear, allowing us, in theory, to validate some solutions and discard others. Another precious tool to validate the interpretation of one of the IFP spot as a result of the precipitation of trans-hemispheric electrons is the qualitative estimate of the different inter-spot distances. I will thus extend quantitatively and detail the conclusions that we reached in the previous chapter.

4.2 Satellites footpaths as constraints for improving Jovian magnetic field models

4.2.1 Models of the internal magnetic field

The idea of using the Io footprint location to constrain the magnetic field models appeared very early in the short story of the Io footprint. Indeed, the concept was proposed as soon as 1993 by *Connerney et al.* when they reported the first observations of the infrared auroral signature of the Io-Jupiter interaction. We must admit that the case of the Io footprint is exceptional in the studies of the aurorae. Whatever the planet under consideration, it has always been a considerable challenge to precisely relate phenomena taking place in the equatorial plane of the magnetosphere and their high latitude auroral counterparts. The problem is that we usually do not know the exact topology of the magnetic field, either because of the lack of observational constraints or because it strongly varies with time (or both, of course). In the case of the satellite footprints, if we neglect the lead angles, the connection between a given position in the magnetosphere and its projection on the planets along magnetic field lines is direct. Io, Europa and Ganymede can then be used as landmarks to estimate the mapping of auroral features on Jupiter. For example, *Radioti et al.* (2009b) made use of tabulated Ganymede footprint locations to discuss the mapping of in situ Galileo observations into the Jovian polar regions (Figure 2.13). The argument also works the other way round: *Radioti et al.* (2008a) used the position of Ganymede's footprint to demonstrate that the discontinuity in

the main emission maps to a region farther than 15 Jovian radii.

We should nevertheless distinguish Io from the other moons because they are not exactly located in the same region of the magnetosphere. Io is only $6R_j$ away from Jupiter and lies in the inner magnetosphere. In this region, the internal magnetic field from Jupiter is by far the dominant contributor to the magnetic field topology. Europa and, to a larger extent Ganymede, being respectively 10 R_j and 15 R_j away from Jupiter, lie in the middle magnetosphere. In this region, the magnetodisk becomes a major contributor to the field. The main effect of this disk of rotating plasma is to stretch the field lines away from Jupiter (see Figure 1.3). The magnetic field models are usually constructed as an "onion" to take these various effects into account. The core of the models represents the inner magnetic field and is usually described as a series expension using magnetic multipoles. Then layers are added, modeling the effect of the different currents flowing in the magnetosphere, like the ring current, the magnetopause currents or the cross tail currents (e.g. *Connerney*, 1981; *Khurana*, 1997;*Alexeev and Belenkaya*, 2005). On one hand, the different contributing currents and their related field contributions vary with time, notably owing to variations of the solar wind conditions. On the other hand, the inner magnetic field is supposed to remain relatively stable[1]. Fortunately, since Io is located in the inner magnetosphere, the influence of these external components is weak. The direct consequence of the above considerations is that the Io footprint can be used directly to constrain the inner magnetic field while we would need to take the ring current and its variations into account if we wanted to use the other footprints. For example, *Grodent et al.* (2008b) found significant latitudinal shifts of the northern main emissions and Ganymede footprint emissions when they compared Jupiter auroral UV images spanning nine years of observation[2]. They showed that variations of the current sheet width and density could explain the latitudinal migration of the emissions.

Anyway, the Ganymede and the Europa footprints had not been discovered when *Connerney et al.* released the VIP4 model in 1998. Previous models were based on least squares fits of in situ magnetic field measurements with spherical harmonics

[1]Comparing magnetic field measurements from Pioneer 11 (that flew by Jupiter in 1974), from Voyager 1 (fly-by: 1979) and from Ulysses (fly-by:1982), *Connerney et al.* (1996) did not notice any significant secular variation of the Jovian internal magnetic field parameters. On the contrary, *Russell et al.* (2001) reported a possible change of the magnitude of the dipole moment on the order of 1.5% from 1975 to 2000 based on Galileo measurements.

[2]The latitudinal variations were respectively on the order of 3° for the main emissions and 2° for the Ganymede footprint.

models. This time, the authors gathered enough IFP position datapoints both from IR and UV observations to reasonably cover the Io footpaths from both hemispheres. In order to find the best model to fit the observations, *Connerney et al.* (1998) computed the radius r_e at which a field line starting at an observed footprint location intercepts the jovigraphic equator for each iteration step. They then used a generalized inverse technique to determine the best 4th degree and order multipole model that simultaneously minimizes the quantity $r_e - r_{Io}$ ($r_{Io} = 5.9R_j$ being the Io's orbit radius) and fits in-situ measurements of the magnetic field from the Pioneer 11 and Voyager 1 spacecraft. Note that the only constraint is that the relevant model field lines reach Io's orbit, but the projected IFP positions are not constrained in longitude. High order terms in the multipole development of the magnetic field essentially affect the surface magnetic field but their influence weakens as the radial distance increases. Consequently only third order and degree terms where constrained by in-situ measurements from Pioneer 10 and 11, Voyager 1 and 2 or even Ulysses probes (e.g. *Connerney et al.*, 1996). Since the IFP projections along modeled field lines provide some information on the surface field, the VIP4 model resolves all but three of the fourth order terms. Of course, a natural consequence of these improvements is that the projection of the Io orbit back to the northern and southern ionospheres is in much better agreement with the IFP data points (Figure 4.1). We should note that the model described in the *Connerney et al.* (1998) paper is composed of two parts: the fourth order and fourth degree spherical harmonic model representing the internal Jovian magnetic field and the magnetodisk magnetic field model described in *Connerney* (1981). The authors applied this two part model to derive expected footpaths for Amalthea as well as for Europa and Ganymede.

Europa and Ganymede footprints have been formally identified in STIS images by *Clarke et al.* (2002) and the large Spring 2007 HST observation campaign considerably increased the available database. *Grodent et al.* (2008a) systematically measured the Io, Europa and Ganymede footprints position and built partial reference contours for these satellites. While the VIP4 predicts contours which are essentially parallel to each other, it is obvious that the observed footpaths diverge from each other in the longitude range from 80° to 150° (Figure 4.2 left). Additionally, images show a hinge in the northern Io tail around 110° longitude that is not reproduced by the VIP4 model. The authors noted that neither the divergence of the footpaths nor the presence of the hinge can be reproduced through a modification of spherical harmonics parameters of order ≤ 4. Additionally, the

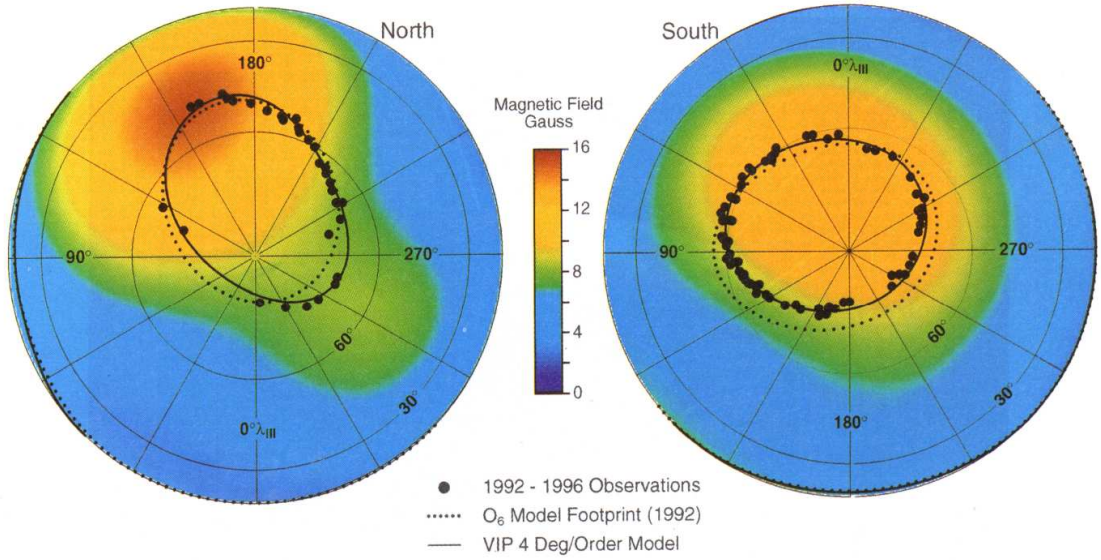

Figure 4.1: Orthographic polar projections of the surface field strength in the northern and southern hemisphere according to the VIP4 model. The polar projection of the Io orbit along the field lines as well as the footprint locations used to build the model are also represented. The projection of the Io orbit along the field lines according to the older O6 magnetic field model is also shown as dashed lines. We can see that the use of Io footprint as a constraint considerably improves the accuracy of the mapping (from *Connerney et al.*, 1998).

potential changes on these parameters should not affect the southern footpaths too much since such a divergence is not observed there. They proposed a novel solution to reproduce the northern footpaths: in addition to modified 3rd and 4th order parameters, their model also encompasses an off-centered dipole situated below the hinge region. Solutions of this kind are not unique and the authors indeed propose two different positions for the dipole that would equally be in accordance with the data. It should also be noted that these two perturbed models are only constrained by northern hemisphere data and do not fit the southern hemisphere footpath. One final comment on these models: the new surface magnetic field maps considerably differ from the VIP4 results (Figure 4.2 right). This observation calls for caution when correlating auroral or low altitude magnetospheric quantities to the magnetic field strength, whatever the model in use.

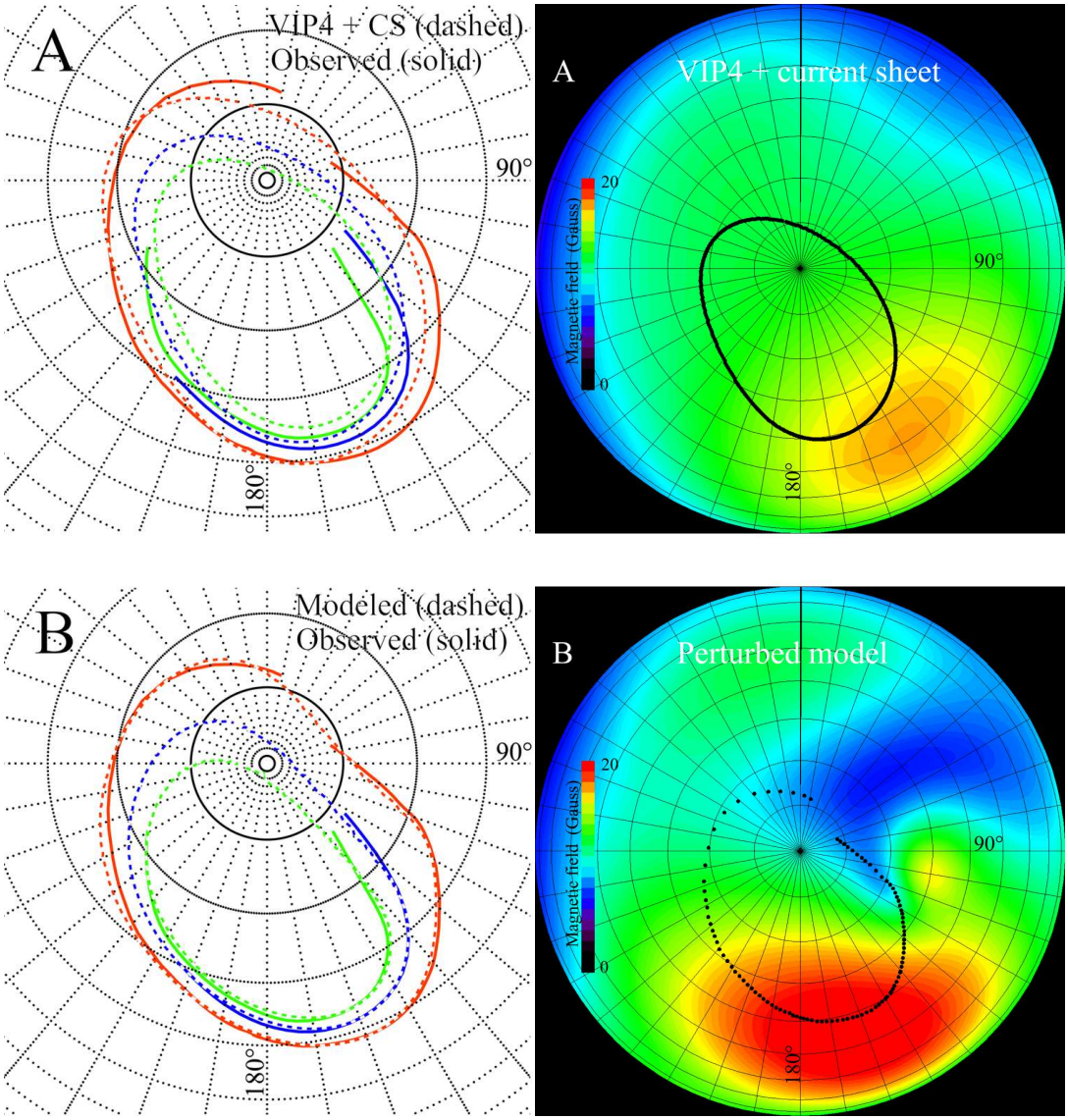

Figure 4.2: (left) The solid lines correspond to the observed contours for the Io (red), Europa (blue) and Ganymede (green) footprints in the northern hemisphere. The colored dashed lines are the projection of the satellites' orbits along the field lines from the VIP4 model (top) and the new model composed of a multipole + a dipole (bottom). It can be seen that the divergence of the observed footpaths is not reproduced by the VIP4 model. (from *Grodent et al.*, 2008a) (right) Polar map of the surface magnetic field intensity for the VIP4 model (top) and one of the alternative models perturbed with an additional dipole (bottom). Both models assume the same magnetodisk model (from *Grodent et al.*, 2008a).

4.3 Location of the Io footprint spots: key observations for validating the interaction models

Most of the material presented in the following section has been published by B. Bonfond, D. Grodent, J.-C. Gérard, A. Radioti, P.A. Delamere, V. Dols and J.T. Clarke under the title: *The Io UV footprint: Location, inter-spot distances and tail vertical extent* in Journal of Geophysical Research - Space Science (*Bonfond et al.*, 2009).

4.3.1 Introduction

The root cause for the Io-Jupiter interaction is the motion of Io with respect to the plasma torus, which generates Alfvén waves propagating along the magnetic field lines that connect Io's neighborhood and Jupiter (see review in *Saur et al.*, 2004). The propagation of these waves has been historically described by two competing models. The first proposed model is called "the steady state unipolar inductor model"(*Goldreich and Lynden-Bell*, 1969) at a time where the existence of neither the Io atmosphere nor the plasma torus had been observationally established. The electric current flowing through Io's atmosphere propagates along field lines to the northern and southern ionospheres of Jupiter, where it closes via the locally horizontal Pedersen current, thus forming a current loop connecting the satellite to the planet. The basic assumption of the model is that an Alfvén wave created at Io would be fast enough to reach the ionosphere of Jupiter and bounce back to intercept Io, establishing this steady current loop. The discovery of the dense plasma torus encompassing the orbit of Io challenged the assumptions of the unipolar inductor model. The high plasma density would slow down tremendously the propagation velocity of the Alfvén wave originating from Io. If this wave retardation is large enough, then, by the time the wave is reflected from Jupiter's ionosphere back to the torus, Io would have had time to slip free from the magnetic flux tube which intercepted it at the time the wave was originally launched.

Consequently, the interaction in this picture is better described in terms of propagation of MHD Alfvén waves which form ideal Alfvén wings. This type of wave carries a current approximately field-aligned, which does not require a closure in Jupiter's ionosphere (*Neubauer*, 1980). Detection by the Galileo spacecraft of a quasi-stagnated flow in the wake of Io, within half an Io radius of the surface (*Frank*

et al., 1996), regenerated interest in the unipolar inductor model in the literature: because of the strongly retarded flow, the Alfvén wave launched at Io could have the time to bounce back from the ionosphere and return to Io, which is the scenario of the unipolar inductor. Several authors recently proposed a formalism where the Alfvén wing model and the unipolar inductor are the two extreme cases of the same interaction (*Crary and Bagenal*, 1997; *Pontius*, 2002; *Saur*, 2004].

In principle, careful observations of the location of the Io spot could determine whether the interaction is better described with either the unipolar or the Alfvén framework, or a potential mix of the two. The distance between the observed IFP auroral emission and the instantaneous projection of Io on the Jovian ionosphere along the field lines is called the "lead-angle". The unipolar inductor model predicts a large lead angle $\geq 12°$, depending on the conductivities of Io and Jupiter but not on the location of Io in the torus. The Alfvén wave model predicts a smaller lead angle $\leq 6°$, independent of the Jovian conductivity but strongly dependent on the local plasma properties through which the Alfvén wave is traveling. Consequently the Alfvén wing model is strongly dependent on Io's latitudinal location in the torus. In both cases, the IFP is expected to occur downstream (along the direction of planetary rotation) of the position of Io as mapped along undisturbed magnetic field lines.

The first estimates of the lead angle were based on IR images and on the O6 magnetic field model (*Connerney et al.*, 1993). They suggested that the lead angle was independent of Io's System III longitude and was as large as 15-20°. These results were in favor of the unipolar inductor. However, *Clarke et al.* (1996)(1998), *Prangé et al.* (1998) and more recently *Gérard et al.* (2006) showed lead angle measurements based on HST FUV observations and on O6 or on VIP4 magnetic field models (*Connerney et al.*, 1998) indicating that the lead angle could vary with Io's longitude and even attain negative values. This later result is particularly puzzling since no model predicts an upstream bending of field lines nor a perturbation which propagates against the rotation of ambient magnetospheric plasma. The occurrence of lag angles was attributed to the lack of accuracy of the magnetic field longitudinal mapping. The VIP4 magnetic field model and its later improvements by *Grodent et al.* (2008a) are built in such a way that the mapping of the Io orbit along the field lines is constrained to fall on the locus of the IFP as seen on IR or UV images (the IFP reference contour). This method brings substantial improvements compared to earlier models which relied only on in-situ magnetic field measurements in the

equatorial plane. However, the longitude along the reference contour is not constrained by the observations. If the magnetic field models were directly linking Io to its northern and southern footprints by construction, then measurements of the lead angle would be meaningless. Nevertheless, it is not clear whether the absence of such a constraint provides more significant information.

Another method to determine the lead angle is based on measurements of the inter-spot distances. If the Alfvénic perturbations remain small compared to the ambient field, then the lead angle is directly linked to these distances. The relationship between secondary spot positions and Io's centrifugal latitude (i.e. latitude with respect to the rotational equator) was first suggested to be caused by reflections of the Alfvén waves on the torus boundaries (*Gérard et al.*, 2006). In this case, the maximum lead angle is expected to correspond to half of the maximum inter-spot distance. However the recent finding of a faint spot appearing upstream of the main emissions puts this interpretation into question. An alternative explanation assumes that the upstream or downstream secondary spots are caused by electron beams originating from the opposite hemisphere (*Bonfond et al.*, 2008). According to this trans-hemispheric electron beams model, when Alfvén waves dissipate their energy in the form of electron parallel acceleration, most electrons are accelerated towards the planet, creating the main Io spot. Part of the electron population, however, is accelerated towards the opposite hemisphere in the form of electron beams. Since these electrons are essentially undisturbed by the torus plasma (unlike the Alfvén waves), they may precipitate upstream or downstream of the other hemisphere's main spot depending on the Io centrifugal latitude. Three spots are defined in this framework: the Main Alfvén Wing spot (MAW spot), the Trans-hemispheric Electron Beam spot (TEB spot) and the Reflected Alfvén Wing spot (RAW spot). Accordingly, the maximum inter-spot distance between the MAW spot and the TEB spot would provide a good estimate of the maximum lead angle. Nevertheless, other models considering a stronger interaction do not predict such obvious relationships between the inter-spot distance and the lead angle. It is not clear how a pure unipolar model could explain the multi-spot structure and the systematic variation of the inter-spot distances. However, *Jacobsen et al.* (2007) suggested that strong non-linearities could trigger wave interference patterns leading to the occurrence of multiple spots and depending on Io's location in the torus.

The large Hubble Space Telescope (HST) campaign dedicated to Jupiter's aurora in Spring 2007 brought a wealth of new data concerning the IFP. Here we describe

the careful determination of the footprint location. We define a new IFP reference contour, and measure the lead angles as well as of the inter-spot distances on an unprecedented longitude coverage.

4.3.2 New Io reference contours

IR and UV observations have shown that the IFP follows a fixed path in S3, called the IFP reference contour. In order to fully determine this contour in each hemisphere, we need images of the IFP spanning all Io S3 longitudes. In previous HST campaigns, the observing geometry was mainly constrained by the visibility of the main auroral emission, systematically leaving some configurations unexplored. The latest ACS observations now fill most of these gaps and provide the missing data points. *Grodent et al.* (2008a) used this more complete ACS dataset to build reference contours for Io, Europa and Ganymede in the northern hemisphere by manually selecting the location of the footprint spots and Io's tail on the images. Following *Grodent et al.* (2008a), we assume the manually selected spots to be located 700 km above the 1 bar level. These observations include configurations where the IFP lies very close to the planetary limb, leading to large inaccuracies. The problem is particularly pronounced in the 350-100° Io S3 sector, where the reference contour does not seem to form a closed curve according to the simple polar projection of the observed footprint location (see Figure 1 in *Grodent et al.* (2008a)). In order to increase the accuracy of the IFP localization in this critical sector, we take advantage of the fact that our observations were designed to acquire images in the same Io S3 longitude but for different local time configurations. The Io S3 longitude difference tolerance between the two observations is as low as 0.25°, which is less than one third of the S3 longitude range covered by Io in 100 s. This means that, for each pair of images, Io is almost in the same position with respect to the Jovian magnetic field, but the footprint is seen from different points of view (with respect to the Jupiter-Earth line of sight). Assuming that the IFP is located exactly at the same place on both images[3], we determine the longitude/latitude couple that minimizes the distances in pixels between the computed point and the manually selected pixel on both images. The new IFP location typically lies within 2-3 pixels of the originally selected position. For example, the uncertainty on the IFP location around 0° Io S3 longitude, which was as large as 5° based on single images,

[3]I.e. assuming that local time and temporal effects are negligeable.

is now reduced down to $\sim 2^\circ$ in longitude and $\sim 1^\circ$ in latitude. In the sectors where such image pairs exist, we only take these new points into account (pale grey triangles in Figure 4.3). In sectors where images pairs are missing, we consider spot locations (dark grey diamonds) or tail locations (black crosses) derived from unique images. We are now in position to construct a new reference contour with a more realistic closure in the northern 30-60° Io S3 longitude range (Figure 4.3 left and Table 4.1). The agreement between our reference contour and the footprint positions measured on high resolution images (from 25.7 km/pixel to 133.7 km/pixel) in the visible wavelength by Galileo (*Vasavada et al.*, 1999) is convincing. We note that, in the North, our reference contour mainly differs from the VIP4 Io contour in the region influenced by the magnetic anomaly between 100 and 180° longitude. Some significant differences also arise between 210° and 290°.

As far as the southern hemisphere is concerned, the Io S3 coverage gaps were even wider than in the North. Most of them are now filled, making it possible to draw an updated southern Io footpath reference (Figure 4.3 right and Table 4.1). The agreement between the VIP4 Io contour and our reference contour is better in the South. Our footpath only lies a few degrees equatorward from the VIP4 contour near 0° and near 90°. Finally, we note that the two contours have very similar lengths: ∼173000 km for the North and ∼167 000 km for the South.

4.3.3 Lead angle and inter-spot distances

Now that we have an accurate relationship between the orbital longitude of Io and the corresponding position of the main IFP spots, computing the lead angles is relatively straightforward provided we have an accurate magnetic field model. In addition to the VIP4 model, we also used the second multipole + dipole model from *Grodent et al.* (2008a) in the North for comparison. It should be noticed that, where the northern contour is very close to the pole, a small distance on the planet corresponds to a large interval when expressed in terms of longitude. Moreover, measuring the longitudinal shift directly on the planet does not enable us to meaningfully compare values from opposite hemispheres nor to verify theoretical predictions since these usually implicitly assume an axisymmetric magnetic field. Consequently, in order to avoid these geometrical effects due to the shape of the contours, we provide measurements of the *equatorial* lead angles. Thus, contrary to *Clarke et al.* (1998) and *Gérard et al.* (2006), we do not magnetically map the

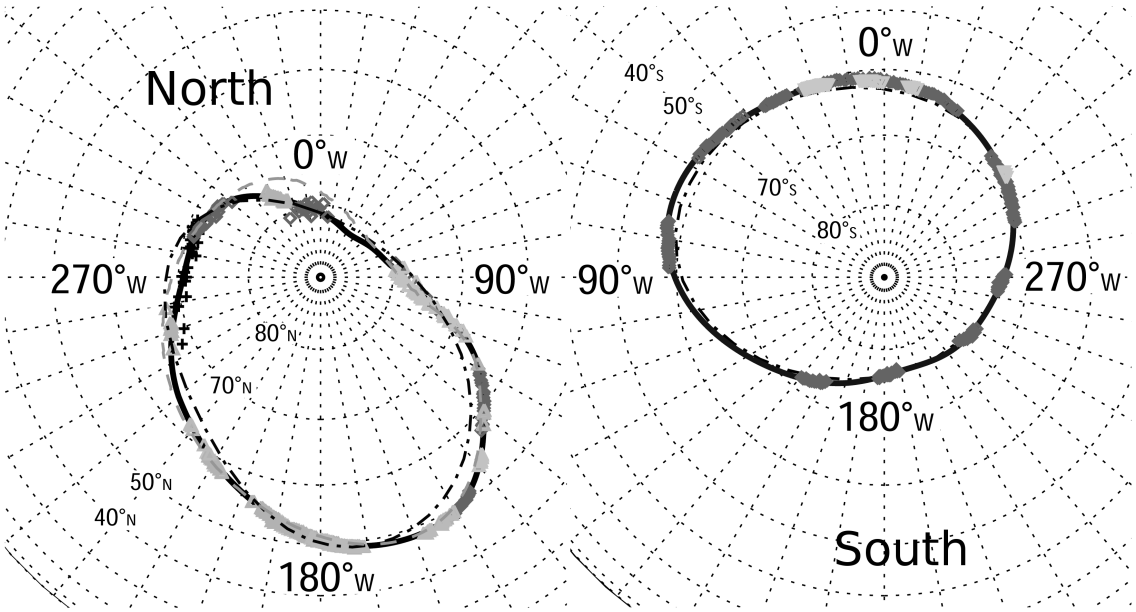

Figure 4.3: Planeto-centric polar projection of the Io reference contours for the northern and the southern hemispheres. The triangles represent IFP locations computed from coupling two images. The rhomboids represent IFP locations deduced from a unique image. The black crosses represent points selected in the IFP tail. The black dash-dotted line is the IFP contour from the VIP4 model, the dashed grey line is the IFP contour from the second model described in *Grodent et al.* (2008a) and the thick plain black line is the best fit to the data points.

Io S3 Longitude (°)	North IFP Longitude (°)	North IFP Latitude (°)	South IFP Longitude (°)	South IFP Latitude (°)
0	-32.0±2	76.9±1	5.1±1	-61.4±1
10	-22.6±5	78.5±1.5	14.1±1	-61.0±1
20	-2.1±7.5	81.0±2	23.2±1	-60.6±1
30	32.7	82.7	32.2±1.5	-60.1±1
40	70.7±3	81.4±2	40.9±1	-59.3±1
50	96.9±2	77.0±1.5	49.2±1	-58.5±1
60	110.1±1	69.3±1.5	56.9±1	-57.7±1
70	118.6±1.5	64.3±1	64.1	-57.3
80	126.3±1.5	60.9±1	71.0	-57.3
90	132.6±1	57.9±1	77.8±1	-57.7±1
100	137.7±1	55.0±1	84.5±1	-58.6±1
110	142.1	52.6	91.3	-60.0
120	145.8±0.5	50.8±1	98.3	-61.8
130	150.0±0.5	49.5±1	105.5	-63.8
140	154.5±0.5	48.8±1	113.2	-66.0
150	158.4±0.5	48.6±1	121.8	-68.1
160	162.7	48.7	131.6	-70.2
170	168.1±0.5	48.9±0.5	143.3±1.5	-72.1±1
180	173.5±0.5	49.5±0.5	156.8±1.5	-73.9±1
190	178.4±0.5	50.4±0.5	172.1±2.5	-75.6±1.5
200	183.2±1	51.7±0.5	188.6±2.5	-76.8±1.5
210	188.5±1	53.3±1	205.4	-76.8
220	194.3±1	55.0±1	221.7	-76.2
230	200.5±1	56.6±1	236.6±1.5	-75.6±1
240	207.5±1	58.5±1	250.1	-75.0
250	214.6±1	60.4±1	262.0±2	-74.2±1
260	220.8±2	61.6±1	272.8±2	-73.0±1
270	228.0±3	63.0±1	282.9	-71.7
280	238.8±1.5	65.1±0.5	292.6±2.5	-70.4±1
290	252.1±1.5	67.7±0.5	302.2±2	-69.0±1
300	265.4	69.8	311.7±1.5	-67.8±1
310	278.4	70.9	321.0±1.5	-66.5±1
320	290.6±5	71.6±1.5	330.0	-65.2
330	301.5±5	72.5±1.5	338.8±1.5	-64.0±1
340	311.6±5.5	73.9±1.5	347.5±1	-62.9±1
350	320.7	75.5	356.3±1	-62.0±1

Table 4.1: Planeto-centric coordinates of the Io northern and southern reference contours. Assuming a selection uncertainty of 3 pixels, the mean geometric uncertainty is provided only when it is constrained by data points.

location of Io to the ionosphere and then measure the longitudinal distance to the actual IFP. Instead, we link the IFP location to the nearest point on the model reference contour and we map this point back to the equatorial plane in order to measure the actual longitudinal shift with respect to Io. Figure 4.4a shows that the equatorial lead angle in the North is strongly model dependent. For example, the inexplicable negative lead angles in the 100° sector disappear when the magnetic mapping is done by the *Grodent et al.* (2008a) model. Figure 4.4b shows that the equatorial lead angle in the South has a more structured behavior, showing a smooth evolution as a function of Io's longitude. Nevertheless, the maximum and the minimum lead angles both appear when Io is in the center of the torus, i.e. close to 110° and 290° S3.

In Figure 4.5, we show the variations of the inter-spot distances for both hemispheres according to the trans-hemispheric electron beam model (see Chapter 3). In this plot, points are marked only when the secondary (and tertiary) spots are clearly observed on the image. The distances are shown in kilometers in order to avoid problems with the contour geometry and the use of magnetic field models. However, in order to provide a rough idea of the distances in terms of longitudinal shift, we can consider that 1° corresponds to ∼470 km (∼480 km in the North and ∼465 km in the South). In the North, the secondary spots are usually fainter than in the South. Thus these spots can only be distinguished from the main one when the inter-spot distance is large enough. However, between 0° and 100° in the southern hemisphere, the secondary spot becomes as bright as the main one and we can follow their merging on the images. The variations of the southern inter-spot distances look regular and correlated with the position of Io in the torus. Additionally, the inter-spot distances in the North and in the South appear to follow a symmetric behavior (see also Figure 3.4).

4.3.4 Discussion

The large amount of data collected during the HST/New Horizons campaign provided images of the Io footprint over a wide range of System III longitudes. *Grodent et al.* (2008a) carefully measured these footprint locations in order to build reference contours for the different satellite footprints in the northern hemisphere. However, the poor accuracy of the IFP locations around 0° S3 made the contour difficult to close in a reasonable way in the 0-60° range. We took advantage of IFP images

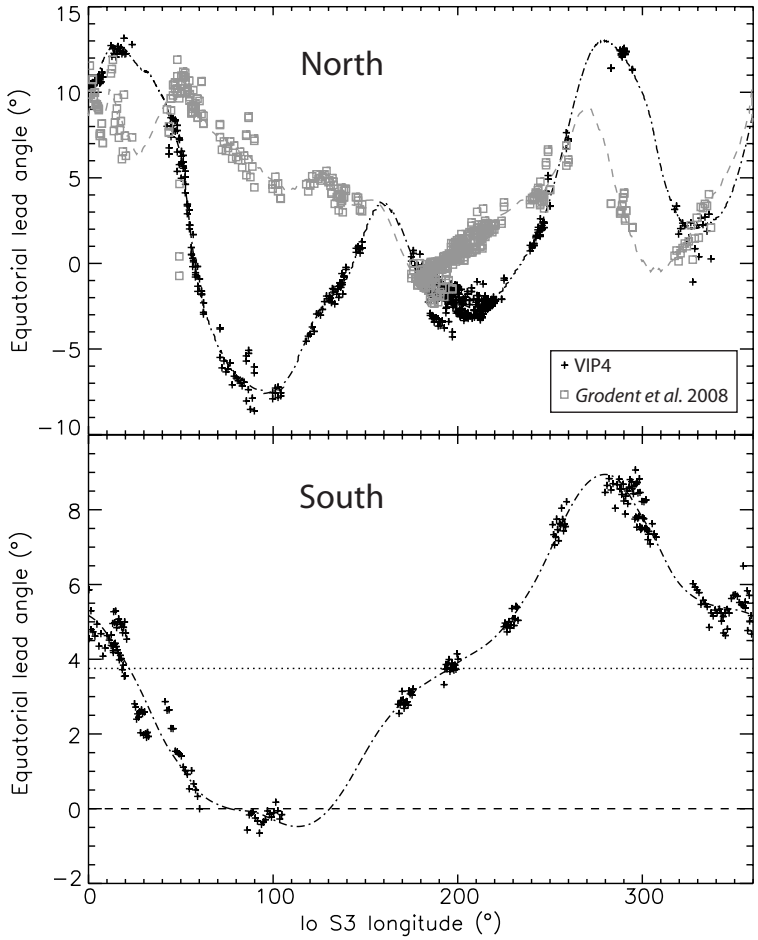

Figure 4.4: Equatorial lead angles for the northern and the southern footprints. The black crosses represent the data points as computed with the VIP4 model while the grey squares represent the equatorial lead angle using mapping from the second multipole+dipole model from *Grodent et al.* (2008a). The black dash-dotted and grey dashed curves are fifth order Fourier series fitting of the data points for the VIP4 and *Grodent et al.* (2008a) models respectively.

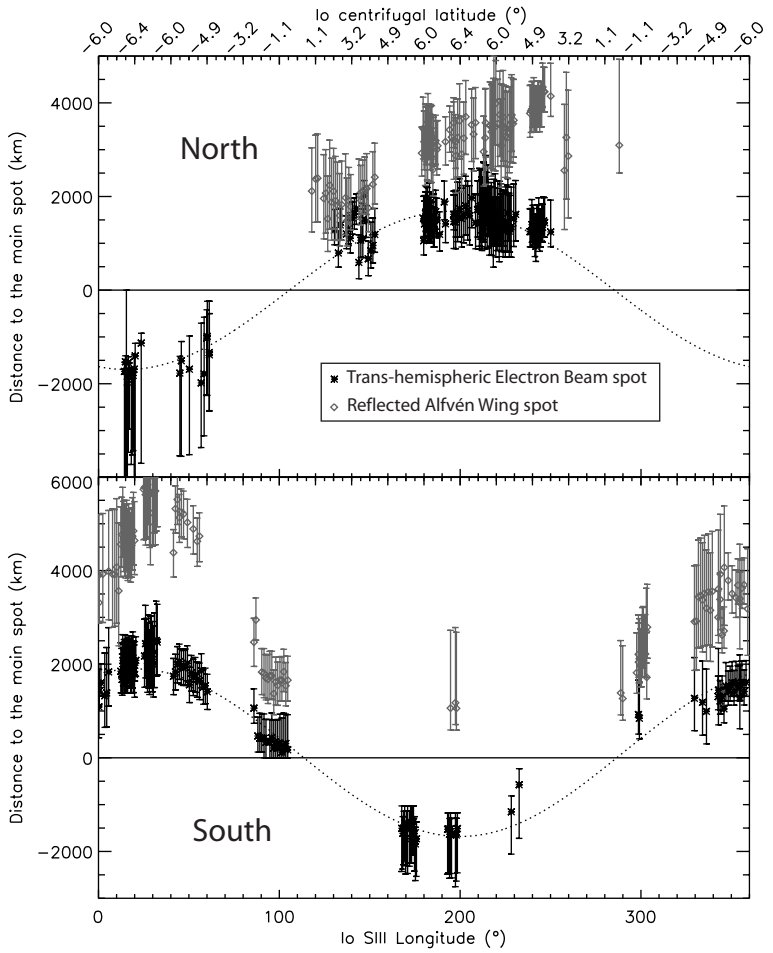

Figure 4.5: Inter-spot distances as a function of the Io S3 longitude of the northern (Top) and the southern hemispheres (Bottom). The error bars are built assuming a selection uncertainty of 1 pixel for the main spot and 2 pixels for the usually fainter secondary spot. The adopted theoretical framework to decide which is the main spot is the same as in *Bonfond et al.* (2008). The two curves correspond to the best fit of the points with a sinusoid function. The maxima lie around 1500-2000 km, which roughly corresponds to 3-4° into the equatorial plane.

with identical Io S3 latitudes but with different local time configurations to precisely locate the IFP for these critical longitudes. Finally, we constructed IFP reference contours for both hemispheres based on these IFP locations.

The new reference contours describing the IFP path were then used to compute the angle between the S3 location of Io and the projection of the IFP along the unperturbed magnetic field lines. Figure 4.4 shows that the lead angles vary with the S3 position of Io but are very model dependent. Additionally, in the northern hemisphere, the lead angles do not organize in a smooth trend, whatever the model. Even though the southern hemisphere curve shows some regularity, it implies that the lead angle when Io is in the dense torus center can vary from $\sim 0°$ to $\sim 9°$. We note that the lead angles vary with Io's longitude but do not follow the ideal Alfvén wing model expectations. In this interpretation framework, the maximum lead angle is supposed to occur when the Alfvén waves have to cross the entire torus, while the minimum value is expected when the Alfvén waves propagate through a relatively short path in the torus. It is thus surprising to find that the lead angle could reach both its minimum and maximum values when Io is exactly in the same position relative to the torus.

These results and the strong model dependence suggest that the current magnetic field models may not be accurate enough to provide trustworthy lead angle estimates. Possibly, future JUNO probe magnetic field observations will have the required precision for such measurements. Furthermore, the fact that inter-spot distances follow symmetric and regular curves when measured directly on the planet strengthens this conclusion. If the Alfvénic disturbance can be assumed to be linear, the inter-spot distances are related to the bending of the Alfvén wing. Then the secondary spot cannot be attributed to Alfvén wing reflections at the plasma torus boundaries because the distance would not be a minimum when Io is in the torus center. Only the trans-hemispheric electron beam scenario could explain the secondary spot behavior. In this case, the lead angle varies with Io's centrifugal latitude, and its maximum value corresponds to the maximum inter-spot distance and lies around 4°. However, Alfvén wing reflections could still account for the third spot as suggested by *Bonfond et al.* (2008). If non-linear wave interactions are significant, then the link between the lead angle and the inter-spot distance is less direct. Further simulations are required to test whether such models can better match the inter-spot distances reported here.

4.3.5 Conclusions

The lead-angle has been traditionally considered as a crucial parameter to test the far field interaction models. As long as the data were sparse, the measured lead angles have been claimed to favor the unipolar inductor model when the estimated value was large ($\sim 15-20°$) (*Connerney et al.*, 1993) or the ideal Alfvén wing model when it was small ($\sim 0-2°$) (*Vasavada et al.*, 1999). When the datasets began to fill out, the picture became more confused and the absence of clear trend was attributed to the lack of accuracy both on the measurements and on the model (*Clarke et al.*, 1998; *Gérard et al.*, 2006). Indeed, the fact that the modeled and observed reference contours do not match well demonstrates the limitations of a possible comparison between modeled and observed IFP positions (see Figure 4.2). But I claim that the problem is worse than that: we are asking magnetic field models, and VIP4 in particular, for information they cannot provide. It is not only a matter of accuracy but also a matter of construction. The VIP4 model and the *Grodent et al.* (2008a) models are built in such a way that the mapping of the Io orbit along magnetic field lines corresponds to an Io footprint reference contour. Even if the contour fit were infinitely accurate, the fact that a model field line passing through Io has its footprint on the Io contour does not guarantee that it will fall at the right place on this contour because the models are not longitudinally constrained. They would only be trustworthy if we could demonstrate that the x^{th} order multipole in use is the exact representation of the Jovian magnetic field.

This argument seems to be confirmed by our measurements of the equatorial lead angles based on the extended image database acquired in the Spring 2007. The variations of the equatorial lead angles as a function of the System III position of Io are found unexpected, erratic and strongly model dependent. This noting sharply contrasts with the smooth and regular evolution of the inter-spots distances and suggests that the current magnetic field models are not sufficiently accurate to provide information on the Alfvén wing's bending.

On the other hand, the inter-spot distances and the centrifugal latitude of Io are correlated, and the behavior of the curves in the northern and southern hemispheres is found symmetric. Whatever the hemishere, the minimum inter-spot distance between the main and the secondary spots is located in the torus center, which suggests that the secondary spot is not attributable to Alfvén wing reflections at the torus boundaries. Simulations of the MAW-TEB inter-spot distances based on density profiles from *Bagenal* (1994) and the VIP4 magnetic field model reproduce very

well the measured inter-spot distances, notably their maximum value (∼2000 km) and the maximum location (S. Jacobsen, private communication). This confirms that the trans-hemispheric electron beams interpretation is fully compatible with our measurements.

4.4 Epilogue

The satellites footprints positions tell us a lot about the Jovian magnetic field. They provide a unique way to get information on the surface magnetic field that was inaccessible from past fly-by and orbiting probes. Because of their direct connection to their related satellite, the Io, Europa and Ganymede footprints provide unique mapping information between the Jovian polar ionospheres and the magnetosphere. For this reason, the Io footprint, and then Europa's and Ganymede's footprints as well, have been used as constraints for improving magnetic field models.

However, the Io footprint location does not only provide information on the Jovian magnetic field, it also helps to understand the Io-Jupiter interaction. A fundamental result of our study is that we now have an accurate knowledge of the IFP location as a function of Io's longitude in the Jovian magnetic field. We can not only predict where the main spot is located, but we can also predict the relative position of the different spots. In addition, we showed that a parameter that was considered for years as the key parameter to validate the far field Io-Jupiter interaction models, the lead angle, is actually not reliable enough to meet this expectation. Hopefully, we demonstrated that the inter-spot distances are a much more useful quantity to discriminate between the models. We found that the trans-hemispheric electron beam model that we proposed in the previous chapter is fully compatible with the present qualitative measurements, contrary to many previous interpretations.

Additionally, the characterization of these position parameters is interesting by itself, but it is also a mandatory step for the next phase of our Io footprint exploration. For example, the new reference contours will be extremely precious to describe the evolution of the tail characteristics with the distance from the main spot. Moreover, the precise spots localization, both on the planet and respective to each other, will also prove to be extremely useful when we study the brightness of the different spots.